

Glycolipids Support E-Selectin-Specific Strong Cell Tethering under Flow

Monica M. Burdick,* Bruce S. Bochner,† Brian E. Collins,‡,¹
Ronald L. Schnaar,‡ and Konstantinos Konstantopoulos*,²

*Department of Chemical Engineering, †Department of Medicine, Division of Clinical Immunology, and ‡Department of Pharmacology and Molecular Sciences, Johns Hopkins University, Baltimore, Maryland 21218

Received April 20, 2001

This study provides functional evidence that glycosphingolipids constitute ligands for E-selectin but not P-selectin. Chinese hamster ovary (CHO) cells expressing E-selectin (CHO-E) or P-selectin (CHO-P) were perfused over $\alpha 2,3$ -sialyl Lewis X ($\alpha 2,3$ -sLe^x) presented as the hexaosylceramide glycosphingolipid adsorbed in a monolayer containing phosphatidylcholine and cholesterol. CHO-E cells tethered extensively and formed slow, stable rolling interactions with $\alpha 2,3$ -sLe^x glycosphingolipid but not with the comparable $\alpha 2,6$ -sLe^x glycosphingolipid. Tethering/rolling varied with wall shear stress, selectin density, and ligand density. In contrast, $\alpha 2,3$ -sLe^x glycosphingolipid supported only limited, fast CHO-P cell rolling. As calculated from a stochastic model of cell rolling, the step size between successive bond releases from the $\alpha 2,3$ -sLe^x glycosphingolipid was smaller for CHO-E than CHO-P cells, whereas the opposite effect was observed for the waiting time between these events. Detachment assays revealed stronger adhesive interactions of CHO-E than CHO-P cells with $\alpha 2,3$ -sLe^x glycosphingolipid. These findings indicate that glycosphingolipids expressing an appropriate oligosaccharide mediate cell tethering/rolling via E-selectin but not P-selectin. © 2001 Academic Press

Key Words: sialyl Lewis^x; selectins; shear.

E-, L-, and P-selectin comprise a family of adhesion proteins that mediate the initial tethering and rolling of leukocytes on stimulated endothelium during an inflammatory response. Each selectin recognizes a

common carbohydrate epitope, the sialyl Lewis x (sLe^x) oligosaccharide (1), but emerging data indicate that each selectin functionally binds to that epitope (or closely related fucosylated sialylated epitopes) in its own particular biochemical context. Therefore, specific criteria must be met for a receptor to be considered a potential natural selectin ligand. As proposed by Varki (2), the potential ligand must be present in the proper place at the proper time; removal or absence of the ligand should prevent interactions; and the ligand should bind with appropriate selectivity and affinity. No human counter-receptor that convincingly satisfies all of the aforementioned criteria has been identified for E-selectin, although $\alpha 2,3$ -sialylation of a terminal Gal, and fucosylation of a GlcNAc, such as found on sLe^x (1, 3, 4), appear to be important for E-selectin binding (5–7). While many glycoconjugates have been reported to bind E-selectin (8–14), it remains unclear which of these are functional ligands *in vivo*.

Growing evidence suggests that glycosphingolipids, in addition to or rather than glycoproteins, may be natural ligands for E-selectin on normal human neutrophils. E-selectin-dependent neutrophil binding is resistant to numerous proteases (9, 12, 15), and purified or synthetic glycosphingolipids bearing the sLe^x epitope support adhesion of transfected cells expressing E-selectin on their surface (6, 16–18). While studies performed under static conditions can provide initial insight into which molecules bind to selectins, dynamic experimental systems where rolling can occur provide data that are more relevant to the flow environment of the vasculature. Rolling is a complex process in which selectin-ligand bonds are constantly being formed (k_{on}) and broken (k_{off}) under the influence of hydrodynamic forces. A recently developed stochastic model of cell rolling treats the individual distances (step sizes) between successive bonds and the time intervals between these bond breakages (waiting times) as random variables, from which the k_{off} of tethering may be calculated if the dissociation kinetics is

This work was supported by a Whitaker Foundation Grant, National Institutes of Health Grant AI45115, National Science Foundation Grant BES 9978160, and a National Science Foundation Graduate Research Fellowship (to M.M.B.).

¹ Current address: The Scripps Research Institute, La Jolla, CA.

² To whom correspondence should be addressed at Department of Chemical Engineering, Johns Hopkins University, 3400 North Charles Street, Baltimore, MD 21218-2694. Fax: (410) 516-5510. E-mail: konst_k@jhu.edu.

known (19). The k_{off} , and therefore step size and waiting time, reflect the strength of the bond to applied forces: longer step sizes and shorter waiting times correspond to higher k_{off} values, and thus weaker ligand-counter-receptor bonds and faster rolling velocities. Although k_{off} rates have been determined for other selectin binding pairs (20–25) and step sizes and waiting times for unknown neutrophil ligands and E-selectin (19), such analysis between E-selectin, P-selectin, and an immobilized glycosphingolipid has not been previously reported.

In this study, we directly compare the ability of glycosphingolipids to support adhesion of E-selectin or P-selectin transfected cells. More specifically, we demonstrate that mixed polar lipid extracts (PLE) isolated from human peripheral blood neutrophils, as well as a synthetic $\alpha 2,3\text{-sLe}^x$ -bearing glycosphingolipid, preferentially support E- but not P-selectin-mediated adhesion under static conditions. These observations provided motivation for comparing the interactions of Chinese hamster ovary cells expressing E-selectin (CHO-E) or P-selectin (CHO-P) with the well-defined $\alpha 2,3\text{-sLe}^x$ glycosphingolipid construct under flow and establishing comparative kinetic binding parameters between the selectins and the glycosphingolipid target.

MATERIALS AND METHODS

Monoclonal antibodies. Murine IgG1 monoclonal antibodies (mAbs) 68-5H11 (anti-E-selectin) and AK-4 (blocking anti-P-selectin) were purchased from PharMingen (San Diego, CA). Mouse IgG1 function-blocking anti-E-selectin mAb (BBIG-E4) was from R&D Systems (Minneapolis, MN). Irrelevant mouse IgG1 (MOPC-21) was obtained from Sigma (St. Louis, MO). R-phycoerythrin-conjugated horse anti-mouse IgG was from Vector Laboratories (Burlingame, CA).

Preparation of polar lipid extracts (PLE). Peripheral blood neutrophils (>98% purity) were isolated from venous blood of human volunteers by Percoll density gradient centrifugation (12), and polar lipids were extracted using established methods (26). Briefly, granulocytes were homogenized in ice-cold water, glycolipids were extracted in chloroform-methanol-water (4:8:3), precipitated proteins were removed by centrifugation, and polar lipids were partitioned into the upper phase of chloroform-methanol-water (4:8:5.6). The resulting PLE was redissolved in chloroform-methanol-water (4:8:3).

Preparation of adhesion molecule-coated surfaces. PLE from neutrophils corresponding to 8×10^6 cells or 6 pmol/well of a standard lipid (synthetic $\alpha 2,3\text{-sLe}^x$ or $\alpha 2,6\text{-sLe}^x$ glycosphingolipids) were adsorbed as an artificial membrane to microwell dishes from 50 μl of 0.5 μM phosphatidylcholine (PC) and 2 μM cholesterol (Avanti Polar Lipids, Alabaster, AL) (27). After 1 h the wells were washed and blocked with 2.5% bovine serum albumin (BSA, Sigma) in Hepes-DMEM for 15 min at 37°C to prevent nonspecific adhesion.

The synthetic sialyl Lewis X glycosphingolipid $\alpha 2,3\text{-sLe}^x$ and its $\alpha 2,6$ -linked NeuAc isomer ($\alpha 2,6\text{-sLe}^x$ glycosphingolipid) were generous gifts of Dr. Brian Brandley (Glycomed, Inc., Alameda, CA) (6). The glycolipids were used at final concentrations of 0.63 to 10 μM in methanol containing 25 μM PC and 25 μM cholesterol. Two microliters of solution containing $\alpha 2,3\text{-sLe}^x$ or $\alpha 2,6\text{-sLe}^x$ glycosphingolipids or the diluent alone was placed in a 5 mm circle in the center of a butanol/ethanol prewashed 35 mm diameter polystyrene suspension culture dish (Corning, Corning, NY) and allowed to evaporate. If

all input glycosphingolipids were deposited onto the target area, the resulting coated region contained 0.38×10^5 to 6.14×10^5 sLe^x glycosphingolipid molecules/ μm^2 . Assuming 15% stable adsorption (17), the coated glycosphingolipid concentration appears to be in the physiological range (16). Dishes were blocked with 1% BSA in Dulbecco's phosphate buffered saline (PBS) for 2 h at 4°C prior to use. Furthermore, soluble E- and P-selectin (R&D Systems) were coated on 35 mm polystyrene tissue culture dishes (Corning) at an optimal concentration of 0.33 $\mu\text{g/ml}$ as described previously (28).

Cells and culture. COS cells were transfected with plasmids expressing E-selectin or P-selectin in the pCDM8 vector (generous gifts of Dr. Stuart Sweidler, Glycomed, Inc.) as previously described (27). Selectin expression on the COS surface was confirmed by flow cytometry (data not shown). Additionally, confluent HUVECs (passaged twice) were stimulated with 10 ng/ml TNF- α (R&D Systems) for 4 h and harvested nonenzymatically (29) for flow cytometric processing (30).

CHO cells stably transfected with full-length E-selectin or with phosphatidylinositol glycan-linked extra-cellular domain of P-selectin, kindly donated by Dr. Christine L. Martens (Affymax, Palo Alto, CA), were maintained in DMEM/F-12 medium (Gibco) supplemented with 5% fetal bovine serum. CHO-E and CHO-P cells were harvested by non-enzymatic means (1 mM EDTA at room temperature (RT)). This method yielded CHO-E cells expressing two to three times as much surface selectin (percent mean relative fluorescence (%MRF) = 205 ± 18) as either CHO-P cells (%MRF for P-selectin = 100) or 4 h TNF- α stimulated HUVECs (%MRF for E-selectin = 63.1 ± 38.1), as measured by flow cytometry ($n \geq 3$) (30). Therefore, in order to directly compare the results of experiments, "low expression" CHO-E cells, with surface selectin density equal to or lower than that found on stimulated HUVECs or CHO-P cells, were generated by harvesting with 0.05% trypsin-EDTA for 10 min at 37°C (Gibco) (%MRF = 55.9 ± 17.4 , Fig. 2A, inset). Cells ($10^6/\text{ml}$) in 0.1% BSA in PBS with Ca^{2+} and Mg^{2+} were stored at 4°C until use. For flow assays, cells were prewarmed to 37°C for 5 min before perfusion.

Static and dynamic adhesion assays. For static adhesion assays, 40,000 selectin-transfected COS cells were added per lipid-coated well and allowed to incubate for 75 min at 37°C. Nonadherent cells were removed by centrifugation, and adherent cells were quantified by measuring released lactate dehydrogenase activity ($A_{340}/\text{min} \times 10^3$) after detergent lysis (27).

In dynamic adhesion assays, cell interactions with the glycosphingolipid-coated surfaces were quantified using a parallel plate flow chamber and a videomicroscopy/digital image processing system (28, 30, 31). Attachment assays were performed by perfusing cells ($10^6/\text{ml}$) for 10 min at wall shear stresses ranging from 0.5 to 1.2 dyn/cm^2 , thereby mimicking the fluid mechanical environment of the microcirculation and postcapillary venules (32). Tethered cells were defined as those that interacted with the substrate for at least 2 s. Rolling velocity was computed as the displacement by the centroid of the cell divided by the time interval of observation (28).

Controlled detachment assays were performed by perfusing cells ($10^6/\text{ml}$) into the flow chamber and allowing them to settle on the substrate under quiescent conditions for 3 min before step-wise increasing the wall shear stress from 0.2 to 32 dyn/cm^2 every 30 s. Adherent cells were defined as those cells remaining in the field of view during the perfusion period relative to the number in the field during the static incubation (9, 31). Additional cells that tethered from the fluid stream onto the field of view during low shear stresses were included in the analysis of adherent cells. Rolling velocities were obtained from cells remaining bound at the end of each 30 s period.

For inhibition experiments, CHO cells were pretreated for 15 min at RT with mAbs (10 $\mu\text{g/ml}$), which were kept present during the flow assays. In selected experiments the addition of 5 mM EDTA in the flow medium was used to assess the role of divalent cations in cell binding.

Data analysis of total tethering versus shear stress. Increasing the shear stress increases the cell flux and thus the number of cells available to bind to the substrate in attachment assays. It is therefore necessary to decouple the convective effects from the binding kinetics of the process (33–35). Briefly, the effective rate of tethering R was shown experimentally to be a linear function of time that could be described by $R = dC_s/dt$, equal to the slope of the linear regression of a total cell tethering (C_s , cells/mm²) versus time (t , min) plot (34). The value of R was divided by the steady cell flow rate within a height h near the dish surface to obtain an expression for the normalized effective rate of tethering ($NR = R/\psi Q'$), where ψ is the steady cell concentration and Q' is the volumetric flow rate in h . The value of h , set equal to one CHO-E cell diameter (34, 35), was measured as $14.5 \pm 0.6 \mu\text{m}$ ($n = 21$) by image processing. The flow rate through h was defined as $Q' = u_p w h$, where u_p is the cell translational velocity near the dish surface (measured as 417 to 1062 $\mu\text{m/s}$ for 0.5 to 1.2 dyn/cm², respectively), and w is the flow channel width (0.5 cm). ψ is obtained by (33, 35): $\psi = (C_o u_t - R)/u_p h + C_o$, where u_t is the cell settling velocity (measured as $0.13 \pm 0.02 \mu\text{m/s}$) and C_o is the bulk cell concentration (10^6 cells/ml).

Stochastic model of cell rolling. Employing the method of Zhao *et al.* (19) allowed for characterization of the CHO-E and CHO-P cell rolling on $\alpha 2,3\text{-sLe}^x$ glycosphingolipid. Briefly, the step size and waiting time, and thus their respective average values \bar{h} and τ_2 were considered to be random variables. The stationary distribution of rolling velocity can be manipulated to obtain the variance of velocity σ_v^2 for exactly identical cells (19)

$$\sigma_v^2 = \frac{\bar{h}^2}{\tau_2} \left(1 + \frac{\sigma_h^2}{\bar{h}^2} \right) \frac{1}{\Delta t},$$

where σ_h^2 is the variance in the step size \bar{h} and Δt is a chosen time window. Over a population of cells displaying some heterogeneity $\sigma_v^2 = \sigma_h^2 + \sigma_{cc}^2$, where σ_h^2 is the variance due to temporal fluctuation (as a first order approximation equal to the velocity variance of the identical cell population above) and σ_{cc}^2 is the variance due to cell-cell heterogeneity. Multiplying by Δt gives (19):

$$\sigma_v^2 \times \Delta t = \frac{\bar{h}^2}{\tau_2} \left(1 + \frac{\sigma_h^2}{\bar{h}^2} \right) + \sigma_{cc}^2 \times \Delta t. \quad [1]$$

The y-intercept of the linear regression of the data [1] and mean velocity can be used to calculate \bar{h} and τ_2 if a value is assumed for the coefficient of variation for step size (σ_h/\bar{h}) (19).

Statistics. Data are expressed as mean \pm SEM. Statistical significance of differences between means was determined by ANOVA. If means were shown to be significantly different, multiple comparisons by pairs were performed by the Tukey test. Values of $P < 0.05$ were considered statistically significant.

RESULTS

Synthetic $\alpha 2,3\text{-sLe}^x$ Glycosphingolipid and Polar Lipid Extracts from Neutrophils Preferentially Support E-Selectin over P-Selectin-Mediated Cell Adhesion under Static Conditions

Fucosylated and sialylated gangliosides on neutrophils have been posited to be functional ligands for E-selectin (12–14). Therefore, static adhesion assays were performed to compare the ability of fucosylated and/or sialylated glycosphingolipids to support E- or P-selectin-mediated cell adhesion *in vitro*. As shown in

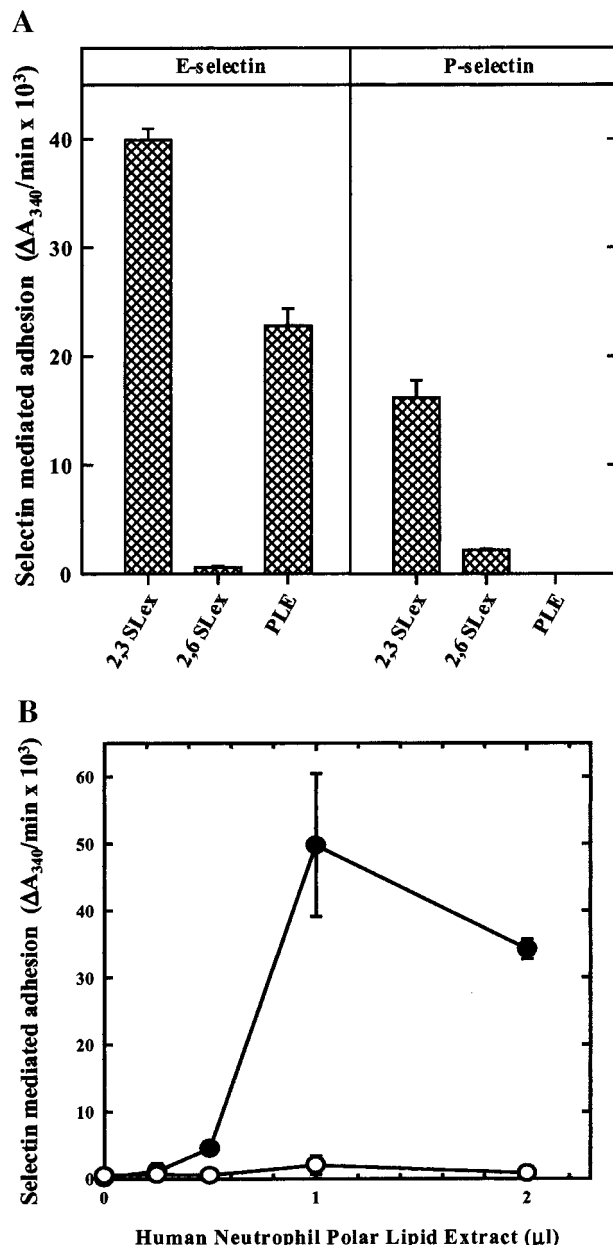


FIG. 1. Adhesion of E- but not P-selectin transfected COS cells to polar lipids from human neutrophils and synthetic $\alpha 2,3\text{-sLe}^x$ glycosphingolipid. (A) COS cells expressing E- or P-selectin were incubated in microwells coated with human neutrophil PLE or the indicated synthetic glycosphingolipids. After centrifugal removal of nonadherent cells, adhesion was quantified by released lactate dehydrogenase activity ($\Delta A_{340}/\text{min} \times 10^3$) from lysed adherent cells. (B) Adhesion of E-selectin (filled circles) or P-selectin (open circles)-transfected COS cells to wells adsorbed with the indicated amount of human neutrophil PLE corresponding to 600,000 cells/ μl was determined as described in A.

Fig. 1A, synthetic sialyl Lewis x (sLe^x) glycosphingolipid with a terminal $\alpha 2,3$ -linked sialic acid supported E-selectin mediated cell adhesion, whereas the same structure bearing a terminal $\alpha 2,6$ -linked sialic acid failed to do so. E-selectin-mediated cell adhesion was

also supported by a mixture of polar lipids extracted from human peripheral blood neutrophils. In addition, treatment of the PLE with neuraminidase, but not the protease trypsin, eliminated binding (data not shown), indicating adhesion was dependent on a protease-resistant, sialic acid-containing neutrophil membrane component(s) such as a glycosphingolipid(s). Compared to E-selectin, P-selectin demonstrated attenuated adhesion to sLe^x glycosphingolipids, and notably failed to support any adhesion to the glycosphingolipid targets extracted from neutrophils (Figs. 1A and 1B). Control cells transfected with plasmid alone did not bind to any glycosphingolipid-absorbed surface (data not shown). We next determined the detailed characteristics of E- and P-selectin-mediated cell adhesion under flow using specific, synthetic glycosphingolipid targets displaying the sLe^x epitope.

$\alpha 2,3$ -sLe^x Glycosphingolipids Support Strong E-Selectin-, but Weak P-Selectin-Mediated Tethering

CHO-E cells expressing either "low" or "high" levels of E-selectin relative to activated HUVECs were perfused over polystyrene surfaces coated with input concentrations from 0.38×10^5 to 6.14×10^5 molecules synthetic sLe^x glycosphingolipid/ μm^2 at 1 dyn/cm². CHO-E cell tethering exhibited concentration dependency of both the coated $\alpha 2,3$ -sLe^x glycosphingolipid and E-selectin expression (Figs. 2A and 2B). Maximal adhesive interactions for both high and low expression CHO-E cells occurred at an $\alpha 2,3$ -sLe^x glycosphingolipid input concentration of 1.54×10^5 molecules/ μm^2 .

Cell tethering was specific since use of an anti-E-selectin blocking mAb abolished binding (Fig. 3). Furthermore, these interactions have an absolute requirement for divalent cations as evidenced by abrogation of attachment upon addition of 5 mM EDTA to the perfusion medium (data not shown). Neither CHO-E nor CHO-P cells interacted with control substrata adsorbed with $\alpha 2,6$ -sLe^x glycosphingolipid or with the carrier lipids alone (PC and cholesterol, data not shown).

CHO-P cells demonstrated a markedly reduced ability to tether to the $\alpha 2,3$ -sLe^x glycosphingolipid compared to CHO-E cells (Fig. 3). Although total tethers of CHO-P cells to the substrate were low, they were specific and divalent cation-dependent, since addition of an anti-P-selectin mAb or 5 mM EDTA to the flow medium abolished tethering (data not shown).

Moreover, substantial differences were observed in the pattern of adhesive interactions. CHO-E cells rolled on the $\alpha 2,3$ -sLe^x glycosphingolipid coated surface (1.54×10^5 molecules/ μm^2 , 1 dyn/cm²) at an average velocity of $\leq 5 \mu\text{m/s}$ (Fig. 3, inset) and demonstrated slow, stable interactions. Under the same conditions, CHO-P cells rolled at $\sim 200 \mu\text{m/s}$ with interactions that were transient in nature (Fig. 3, inset).

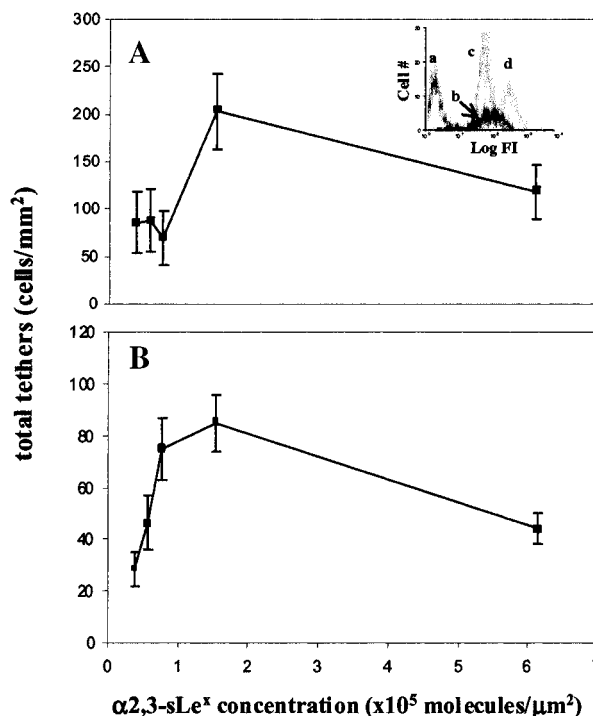


FIG. 2. Effect of $\alpha 2,3$ -sLe^x concentration on tethering of CHO cells expressing (A) high levels and (B) low levels of E-selectin. CHO-E cells were perfused over polystyrene dishes coated with $\alpha 2,3$ -sLe^x glycosphingolipid at the indicated input concentrations at 1 dyn/cm². Tethered cells were those that interacted with the substrate for at least 2 s. Values are mean \pm SEM ($n = 3-8$). Inset, representative FACS profiles of CHO cells expressing P- or E-selectin. FI, fluorescence intensity. (a) IgG control, (b) CHO-P, (c) low expression CHO-E, and (d) high expression CHO-E.

Although CHO-P rolling was rapid, the rolling velocity was substantially lower than the hydrodynamic velocity of a free-flowing cell ($\sim 950 \mu\text{m/s}$). There was no statistical difference in the rolling velocities of high versus low expression CHO-E cells over the ligand concentrations examined at 1 dyn/cm².

Normalization of Shear Stress-Dependent Tethering

To examine the effects of shear on cell tethering, CHO-E cells were perfused over dishes coated with 1.54×10^5 $\alpha 2,3$ -sLe^x glycosphingolipid molecules/ μm^2 at shear stresses ranging from 0.5 to 1.2 dyn/cm². Since the extent of cell tethering increased linearly with the perfusion time (Fig. 4, inset), the effective rate of tethering R was calculated as described under Materials and Methods. Our data show that there was a trend of steady increase for the total amount and thus the effective rate of tethering of low expression CHO-E cells as shear stress increased from 0.5 to 1.0 dyn/cm² (Fig. 4A). However, by increasing the shear stress (flow rate), the cell flux and thus the number of cells available to bind to the coated substrate increase. To decouple the binding kinetics from the convective prop-

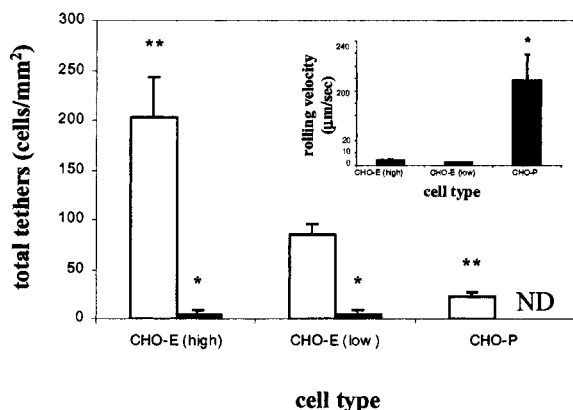


FIG. 3. CHO-E and CHO-P cell tethering on $\alpha 2,3\text{-sLe}^x$ glycosphingolipid. CHO-E and CHO-P cells were perfused over $\alpha 2,3\text{-sLe}^x$ glycosphingolipid-adsorbed surfaces (1.54×10^5 molecules/ μm^2 input concentration) at 1 dyn/cm² and the total number of tethers was quantified in the absence (open bars) or presence of a function blocking E-selectin mAb (closed bars). * $P < 0.05$ with respect to untreated cells, ** $P < 0.05$ with respect to untreated low expression CHO-E cells. Values are mean \pm SEM ($n = 3\text{--}8$). ND, not done. Inset, average rolling velocities were computed as described under Materials and Methods. * $P < 0.05$ with respect to CHO-E cells. Values are mean \pm SEM of 15–65 cells.

erties of the process, we calculated the normalized effective rate of tethering NR by dividing R by the steady cell flow rate near the surface (33, 35). NR for low expression CHO-E cells decreased with increasing shear stress (Fig. 4B). Similar results were obtained for high expression CHO-E cells (data not shown).

Estimation of Step Size and Waiting Times from Rolling Velocities

The rolling velocity means and variances of low and high expression CHO-E cells and CHO-P cells observed

at 1 dyn/cm² on surfaces adsorbed with 1.54×10^5 $\alpha 2,3\text{-sLe}^x$ glycosphingolipid molecules/ μm^2 were analyzed using a model developed by Zhao *et al.* (19). Experimental data fit the model [1] well, with R^2 values near or greater than 0.9 (Fig. 5, representative of all data). Based on the calculated mean velocities and variances and assuming the coefficient of variance step size $\sigma_h/\bar{h} = 0.5$ (19), the value of \bar{h} was determined to be $\sim 0.3 \mu\text{m}$ for both low and high expression CHO-E cells and $\sim 8 \mu\text{m}$ for CHO-P cells. Average waiting times (τ_2) were 0.11 and 0.04 s for CHO-E and CHO-P cells, respectively. These values are in agreement with the observation that CHO-E cells rolled much slower on this substrate than CHO-P cells.

For comparison, neutrophils were perfused over immobilized E- or P-selectin, and their rolling velocities at 2 dyn/cm² were analyzed using the same stochastic model (at 1 dyn/cm², neutrophils did not roll, presumably due to a high selectin concentration). The step size of neutrophil-E-selectin was determined to be $\sim 0.4 \mu\text{m}$ and the waiting time was ~ 0.16 s. Calculations for neutrophil-P-selectin rolling revealed that the step size was $\sim 0.5 \mu\text{m}$ and the waiting time was ~ 0.04 s. The rolling velocity of neutrophils on E- versus P-selectin was measured as 6.0 and 12.5 $\mu\text{m/s}$, respectively.

Resistance to Detachment by Shear Stress

Detachment assays were performed to compare the adhesive strength of interactions between high or low expression CHO-E cells or CHO-P cells and $\alpha 2,3\text{-sLe}^x$ glycosphingolipids. CHO-E cells were much more shear stress resistant than CHO-P cells (Fig. 6A), and the extent of cell detachment was dependent on E-selectin density. The increase in adhesion of CHO-E cells at low shear stress (up to 1 dyn/cm²) was due to cell tethering from the fluid stream, a phenomenon

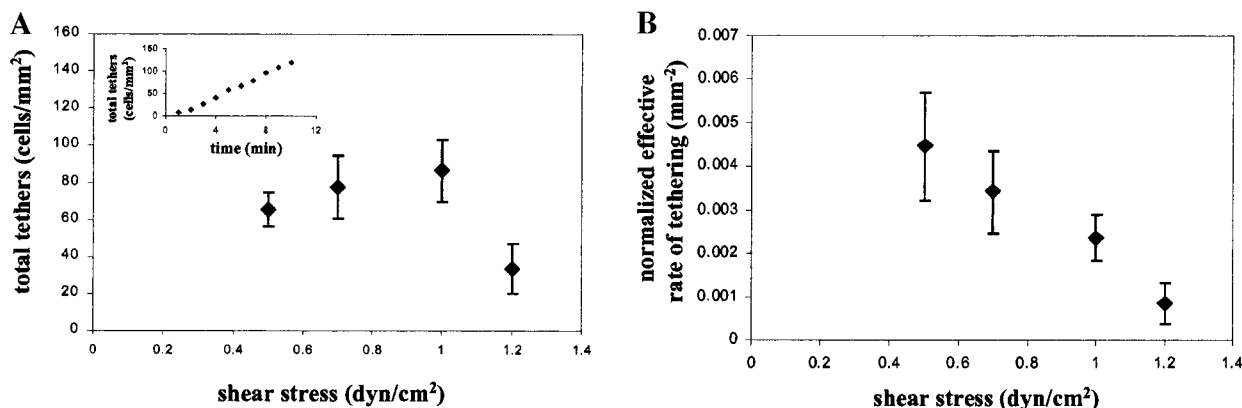


FIG. 4. Normalization of shear stress-dependent tethering. (A) CHO-E (low) cells were perfused over an $\alpha 2,3\text{-sLe}^x$ glycosphingolipid coated dish (1.54×10^5 molecules/ μm^2 input concentration) at shear stresses ranging from 0.5 to 1.2 dyn/cm². Values represent the extent of cell tethering and are mean \pm SEM ($n = 4$). Inset, CHO-E cell tethering to $\alpha 2,3\text{-sLe}^x$ glycosphingolipid at 1 dyn/cm² is a linear function of time ($R^2 = 0.996$), representative of the tethering for both high and low expressing CHO-E cells at different shear stresses. (B) The normalized effective rate of cell tethering, NR, was calculated from the data in A as described under Materials and Methods. Values are mean \pm SEM ($n = 4$).

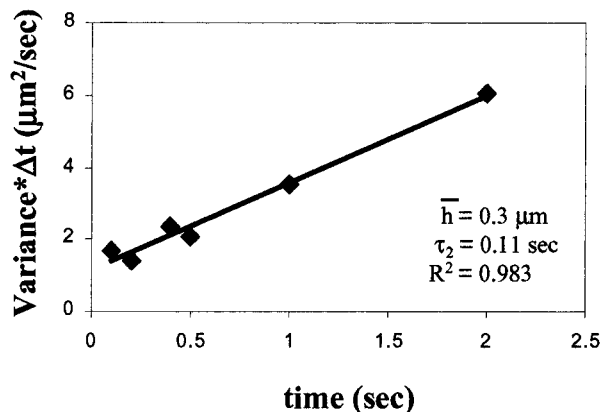


FIG. 5. Calculation of step size and waiting time using a stochastic model of rolling. High expression CHO-E cells ($n = 12$) rolling on $\alpha 2,3$ -sLe^x glycosphingolipid-coated dishes (1.54×10^5 molecules/ μm^2 input concentration) at 1 dyn/cm² were monitored for 2 s. Individual points were calculated from smaller time intervals Δt from the same 2 s total observation period. A least-squares linear regression allowed determination of step size and waiting time of E-selectin- $\alpha 2,3$ -sLe^x glycosphingolipid mediated rolling.

more frequent for high than for low expression CHO-E cells. Complete cell detachment of low-expression CHO-E cells was achieved at 16–32 dyn/cm², whereas only a few high expression CHO-E cells detached even at this level. In marked contrast, ~95% of the CHO-P cells were removed at the lowest shear stress tested. None of the three cell types adhered to the control carrier lipid-coated dishes, with essentially complete cell removal at 0.2 dyn/cm².

Rolling velocities acquired during detachment assays varied with both E-selectin expression and wall shear stress (Fig. 6B). High expression CHO-E cells supported slower rolling that was less sensitive to

shear stress compared to low expression CHO-E cells. However, differences in behavior were only noticeable starting at 2 dyn/cm².

DISCUSSION

In this study we demonstrated that glycosphingolipids favor attachment of E-selectin over P-selectin expressing cells under both static and flow conditions. Namely, in static adhesion assays, PLE from normal human peripheral blood neutrophils containing various fucosylated and/or sialylated glycolipid structures supported sialic acid-dependent E-selectin-, but not P-selectin-mediated cell adhesion. This finding adds to the growing line of evidence that neutrophil glycosphingolipids function in cell-cell adhesion and could act as the natural ligand(s) for E-selectin (6, 9, 12, 15–18). Furthermore, a defined synthetic glycosphingolipid bearing $\alpha 2,3$ -sLe^x also preferentially supported E-rather than P-selectin-mediated binding. These results from static adhesion experiments provided motivation for subsequent dynamic adhesion assays simulating *in vivo* flow characteristics.

Because of the crude nature of the neutrophil PLE, flow-based assays of selectin-glycosphingolipid binding were performed using a synthetic glycosphingolipid structure to isolate adhesion to a single target counter-receptor, forming a well-defined receptor-ligand pair from which adhesion characteristics could clearly be ascertained. This system revealed that the sLe^x epitope displayed on a glycosphingolipid clearly distinguishes between E- and P-selectin in supporting rolling in a model of heterotypic cell-cell recognition and adhesion. Consistent with previous reports (16, 18), tethering and rolling of both types of CHO cells were

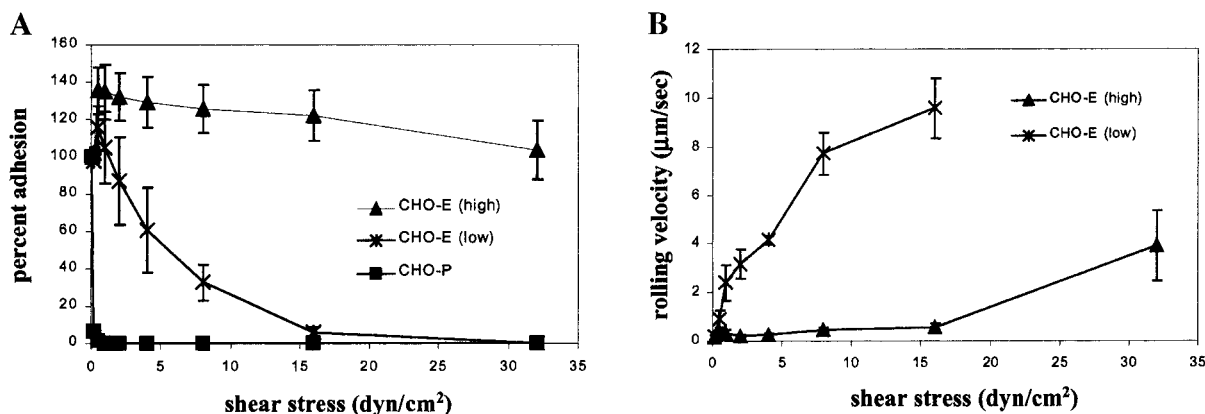


FIG. 6. CHO-E and CHO-P cell detachment from $\alpha 2,3$ -sLe^x glycosphingolipid. (A) Comparison of resistance to shear stress in detachment assays using CHO-E and CHO-P cells. CHO-E and CHO-P cells were perfused over $\alpha 2,3$ -sLe^x glycosphingolipid-adsorbed plates (1.54×10^5 molecules/ μm^2 input concentration) for 30 s, at which time flow was stopped for 3 min. Flow was then resumed, increasing shear stress step-wise every 30 s from 0.2 to 32 dyn/cm². Percent adhesion is indicated relative to the number of cells in the field of view at the end of the static incubation period. Values are mean \pm SEM ($n = 3$). (B) Effect of shear stress on CHO-E cell rolling velocities. Experimental conditions were as in A. Values are mean \pm SEM ($n = 12$ –20 cells).

supported on $\alpha 2,3\text{-sLe}^x$ but not on $\alpha 2,6\text{-sLe}^x$ glycosphingolipid, and the interactions were specific and divalent cation-dependent. Tethering occurred randomly on the substrate, suggesting that the glycolipid coating was fairly uniform and stable, which was verified by fluorescence microscopy (data not shown). Furthermore, CHO-E cell tethering was a function of shear stress, cell surface selectin density, and the concentration of immobilized $\alpha 2,3\text{-sLe}^x$ glycosphingolipid. However, CHO-E cell rolling velocity was not dependent on any of these factors at shear stresses $< 2 \text{ dyn/cm}^2$. It is possible that the densities of $\alpha 2,3\text{-sLe}^x$ glycosphingolipid and/or E-selectin in our experiments were too high to observe differences in rolling velocity at these low wall shear stresses, since it is more sensitive at low selectin-ligand densities, most likely due to the fewer number of bonds (36). When shear stress was increased to $\geq 2 \text{ dyn/cm}^2$ in detachment assays, rolling velocities became dependent on E-selectin density, demonstrating a relatively high strength of adhesion.

In contrast, CHO-P cells tethered much less efficiently and rolled much faster than CHO-E cells even under modest flow conditions. To ensure that the CHO-P cells used in our experiments were capable of sustaining stable interactions when the appropriate ligand (e.g., PSGL-1) is present, CHO-P cells were perfused over a confluent neutrophil monolayer (> 6000 neutrophils/ mm^2) plated on a 35 mm tissue culture dish. CHO-P cells successfully tethered to and rolled on the surface-adherent neutrophils with a mean velocity approximately ten times slower than that on $\alpha 2,3\text{-sLe}^x$ glycosphingolipid (data not shown). Therefore, the low number of interactions between CHO-P cells and the glycolipid-coated substrate was the result of a reduced interaction of P-selectin with $\alpha 2,3\text{-sLe}^x$ glycosphingolipid, and not any failure of the CHO-P cells to bind native ligand. Furthermore, reduced CHO-P interactions were not the result of a lower surface selectin density compared to CHO-E cells, in that CHO-E cells with expression higher and lower than that of CHO-P showed much more robust tethering/rolling on $\alpha 2,3\text{-sLe}^x$ glycosphingolipid.

Previous work has shown that cell binding decreases with increasing shear stress (16, 37). In our study, the raw data of tethering versus shear stress did not reveal this result over the entire shear range tested, implying that convective effects could be obscuring the shear stress dependence. Since more cells are delivered to the flow chamber with the higher flow rates corresponding to increased shear stresses, a normalization method is crucial in order to deconvolute the effects of binding kinetics and transport properties (33, 35). A decrease in the effective rate of tethering as shear stress increased became apparent only after applying the correction for convective effects.

In addition to examining the basic tethering interactions, we also studied the fundamental selectin- $\alpha 2,3\text{-sLe}^x$

sLe^x glycosphingolipid bond in rolling through a stochastic model. The intrinsic random nature of rolling, reflected by fluctuation in rolling velocity observed over a selected time window, was captured by the average step size \bar{h} and waiting time τ_2 between these steps (19) and could be attributed to cell topology, receptor distribution, and/or the inherent stochastic nature of the actual ligand-counter-receptor binding (19). Neutrophil \bar{h} and τ_2 on E-selectin were found to agree with those reported in the literature (19), and those for CHO-E- $\alpha 2,3\text{-sLe}^x$ glycosphingolipid rolling determined in this study. For neutrophil rolling on P-selectin, τ_2 was essentially equal to that for CHO-P- $\alpha 2,3\text{-sLe}^x$ glycosphingolipid but \bar{h} was much smaller. This discrepancy is attributed to the fact that the glycosphingolipid lacks the sulfated residues that enhance P-selectin binding. Altogether, these findings are in concert with published data showing that E-selectin mediates slower rolling of neutrophils than P-selectin (21, 22, 37). Furthermore, if the dissociation kinetics of bond breakage were known to be first order, the dissociation rate constant k_{off} would be the reciprocal of τ_2 . However, we predict that the binding occurring in our system involves multiple bond clusters, in which the relationship between k_{off} and τ_2 would be more complex.

This study is the first to directly compare the abilities of E-selectin and P-selectin to bind a sLe^x -bearing glycosphingolipid under flow conditions. Taken together with the results of static adhesion assays involving both synthetic glycosphingolipids and neutrophil PLE, the data indicate that glycosphingolipids are preferential ligands for E-selectin, in accord with previous work suggesting that glycolipids are the natural ligands for this selectin (13, 14). However, the glycolipid conjugate used in these perfusion experiments was very simple. The results are not meant to suggest that this construct is the naturally occurring leukocyte ligand for E-selectin but rather that an sLe^x -decorated glycolipid can support selective adhesion to E-selectin. It is probable that the ligand is a more complicated lipid structure and has additional binding and/or non-binding epitopes that may critically effect dynamic adhesive interactions such as rolling (18). It is also possible that the E-selectin ligand is an unusual protease-insensitive glycoprotein. Regardless, the data presented herein support the notion that efforts to identify the natural E-selectin ligand on normal human leukocytes should include glycosphingolipids in the analysis. Identification of the ligand would provide a rational basis for developing effective novel therapeutic agents against inflammation.

ACKNOWLEDGMENTS

The authors thank Dr. Brian Brandley (Glycomed, Inc.) for the gift of $\alpha 2,3\text{-}$ and $\alpha 2,6\text{-sLe}^x$ glycosphingolipids, Dr. Stuart Sweidler (Gly-

comed, Inc.) for the gift of selectin transfection vectors, Dr. Christine L. Martens (Affymax) for the gift of CHO cells, Dr. Alka Vyas for assistance with fluorescence microscopy, and Sherry A. Hudson for assistance with HUVEC cultures.

REFERENCES

1. Foxall, C., Watson, S. R., Dowbenko, D., Fennie, C., Lasky, L. A., Kiso, M., Hasegawa, A., Asa, D., and Brandley, B. K. (1992) *J. Cell. Biol.* **117**, 895–902.
2. Varki, A. (1997) *J. Clin. Invest.* **99**, 158–162.
3. Polley, M. J., Phillips, M. L., Wayner, E., Nudelman, E., Singhal, A. K., Hakomori, S., and Paulson, J. C. (1991) *Proc. Natl. Acad. Sci. USA* **88**, 6224–6228.
4. Zhou, Q., Moore, K. L., Smith, D. F., Varki, A., McEver, R. P., and Cummings, R. D. (1991) *J. Cell. Biol.* **115**, 557–564.
5. Walz, G., Aruffo, A., Kolanus, W., Bevilacqua, M., and Seed, B. (1990) *Science* **250**, 1132–1135.
6. Tyrrell, D., James, P., Rao, N., Foxall, C., Abbas, S., Dasgupta, F., Nashed, M., Hasegawa, A., Kiso, M., Asa, D., *et al.* (1991) *Proc. Natl. Acad. Sci. USA* **88**, 10372–10376.
7. Berg, E. L., Robinson, M. K., Mansson, O., Butcher, E. C., and Magnani, J. L. (1991) *J. Biol. Chem.* **266**, 14869–14872.
8. Picker, L. J., Warnock, R. A., Burns, A. R., Doerschuk, C. M., Berg, E. L., and Butcher, E. C. (1991) *Cell* **66**, 921–933.
9. Lawrence, M. B., Bainton, D. F., and Springer, T. A. (1994) *Immunity* **1**, 137–145.
10. Goetz, D. J., Greif, D. M., Ding, H., Camphausen, R. T., Howes, S., Comess, K. M., Snapp, K. R., Kansas, G. S., and Luscinskas, F. W. (1997) *J. Cell. Biol.* **137**, 509–519.
11. Steegmaier, M., Levinovitz, A., Isenmann, S., Borges, E., Lenter, M., Kocher, H. P., Kleuser, B., and Vestweber, D. (1995) *Nature* **373**, 615–620.
12. Bochner, B. S., Sterbinsky, S. A., Bickel, C. A., Werfel, S., Wein, M., and Newman, W. (1994) *J. Immunol.* **152**, 774–782.
13. Stroud, M. R., Handa, K., Salyan, M. E., Ito, K., Lavery, S. B., Hakomori, S., Reinhold, B. B., and Reinhold, V. N. (1996) *Biochemistry* **35**, 770–778.
14. Stroud, M. R., Handa, K., Salyan, M. E., Ito, K., Lavery, S. B., Hakomori, S., Reinhold, B. B., and Reinhold, W. N. (1996) *Biochemistry* **35**, 758–769.
15. Larsen, G. R., Sako, D., Ahern, T. J., Shaffer, M., Erban, J., Sajer, S. A., Gibson, R. M., Wagner, D. D., Furie, B. C., and Furie, B. (1992) *J. Biol. Chem.* **267**, 11104–11110.
16. Alon, R., Feizi, T., Yuen, C. T., Fuhlbrigge, R. C., and Springer, T. A. (1995) *J. Immunol.* **154**, 5356–5366.
17. Larkin, M., Ahern, T. J., Stoll, M. S., Shaffer, M., Sako, D., O'Brien, J., Yuen, C. T., Lawson, A. M., Childs, R. A., Barone, K. M., *et al.* (1992) *J. Biol. Chem.* **267**, 13661–13668.
18. Gege, C., Vogel, J., Bendas, G., Rothe, U., and Schmidt, R. R. (2000) *Chemistry* **6**, 111–122.
19. Zhao, Y., Chien, S., and Skalak, R. (1995) *Biophys. J.* **69**, 1309–1320.
20. Alon, R., Hammer, D. A., and Springer, T. A. (1995) *Nature* **374**, 539–542.
21. Alon, R., Chen, S., Puri, K. D., Finger, E. B., and Springer, T. A. (1997) *J. Cell. Biol.* **138**, 1169–1180.
22. Smith, M. J., Berg, E. L., and Lawrence, M. B. (1999) *Biophys. J.* **77**, 3371–3383.
23. Nicholson, M. W., Barclay, A. N., Singer, M. S., Rosen, S. D., and van der Merwe, P. A. (1998) *J. Biol. Chem.* **273**, 763–770.
24. Mehta, P., Cummings, R. D., and McEver, R. P. (1998) *J. Biol. Chem.* **273**, 32506–32513.
25. Poppe, L., Brown, G. S., Philo, J. S., Nikrad, P. V., and Shah, B. H. (1997) *J. Amer. Chem. Soc.* **119**, 1727–1736.
26. Schnaar, R. L. (1994) *Methods Enzymol.* **230**, 348–370.
27. Collins, B. E., Yang, L. J., and Schnaar, R. L. (2000) *Methods Enzymol.* **312**, 438–446.
28. McCarty, O. J. T., Mousa, S. A., Bray, P. F., and Konstantopoulos, K. (2000) *Blood* **96**, 1789–1797.
29. Kaiser, J., Bickel, C. A., Bochner, B. S., and Schleimer, R. P. (1993) *J. Pharmacol. Exp. Ther.* **267**, 245–249.
30. Konstantopoulos, K., Kukreti, S., Smith, C. W., and McIntire, L. V. (1997) *J. Leukoc. Biol.* **61**, 179–187.
31. Tachimoto, H., Burdick, M. M., Hudson, S. A., Kikuchi, M., Konstantopoulos, K., and Bochner, B. S. (2000) *J. Immunol.* **165**, 2748–2754.
32. Konstantopoulos, K., Kukreti, S., and McIntire, L. V. (1998) *Adv. Drug Deliv. Rev.* **33**, 141–164.
33. Munn, L. L., Melder, R. J., and Jain, R. K. (1994) *Biophys. J.* **67**, 889–895.
34. Dickinson, R. B., Nagel, J. A., McDevitt, D., Foster, T. J., Proctor, R. A., and Cooper, S. L. (1995) *Infect. Immun.* **63**, 3143–3150.
35. Mohamed, N., Rainier, T. R., Jr., and Ross, J. M. (2000) *Biotechnol. Bioeng.* **68**, 628–636.
36. Brunk, D. K., and Hammer, D. A. (1997) *Biophys. J.* **72**, 2820–2833.
37. Kitayama, J., Fuhlbrigge, R. C., Puri, K. D., and Springer, T. A. (1997) *J. Immunol.* **159**, 3929–3939.